Journal of Nepal Hydrogeological Association (JNHA), Vol (3), 102-118 (2026)
ISSN: 3059-9725 (Online)
https://doi.org/10.3126/jnha.v3i1.99535
RESEARCH ARTICLE

Identification of groundwater potential in deep aquifer using electrical resistivity tomography in the Tibetan Tethys of Nepal Himalaya in Korala Naka (Nepal–China border), Mustang district

***Sunil Shankar Pradhananga & Shahid Muslim**
Three D Consultants Pvt. Ltd., Kathmandu, Nepal
**Corresponding author: mallasunil12@gmail.com*
***(Submission Date**: 12 June, 2026; **Accepted Date:** 25 August, 2026)*

ABSTRACT

Reliable groundwater resources are essential for sustainable water supply in the high-altitude, arid environment of Upper Mustang, where surface water is limited and highly seasonal. To assess groundwater potential for this remote, high-altitude community, and two 720 m Electrical Resistivity Tomography (ERT) profiles were acquired parallel to each other using 60 stainless-steel electrodes spaced 12 m apart in a Wenner-array configuration. The inverted sections extend to a nominal depth of approximately 110 m, although the effective depth of investigation and resolution decrease toward the base of the models. After processing the apparent-resistivity data in RES2DINV, the inversions produced RMS errors of 8.2% and 9.4% for Profiles 1 and 2, respectively. Both profiles show a thin, relatively resistive surface zone (approximately 600–1400 Ωm) overlying broad low- to moderate-resistivity zones (approximately 30–350 Ωm) in the central to lower sections. In the context of the local Tethyan Himalayan geology, these lower-resistivity zones are interpreted as potentially water-bearing and may correspond to saturated fine-grained sediment, weathered material, or fractured sedimentary rock such as shale, mudstone, or sandstone/Limestone. However, resistivity responses are non-unique, and clay-rich or poorly connected materials may produce similar signatures without constituting productive aquifers. Because no borehole, lithological log, water-level, or pumping-test data are available for calibration in the Nepalese Tethyan Himalaya, the study does not confirm aquifer productivity, recharge, hydraulic connectivity, or sustainable yield. The results should therefore be regarded as a preliminary geological and hydro-geophysical assessment that identifies priority targets for exploratory drilling and hydrogeological testing to support future water-supply planning for border infrastructure and nearby communities.

Keywords: ***ERT, groundwater exploration, Tethys Himalaya, Trans-Himalayan aquifer, upper Mustang***

INTRODUCTION

Groundwater represents a critical, naturally filtered source of drinking water, essential for sustaining ecosystems and human settlements, particularly in regions where surface water is scarce or seasonal. In the high-altitude, arid environments of the Trans-Himalaya, water security is a mounting concern due to the combined effects of climate change, increasing human activity, and the inherent limitations of surface water sources (Shrestha & Aryal, 2011).

The Tethys (Tethyan) Himalaya, the northernmost tectono-stratigraphic zone of the Nepal Himalaya, extends from western Nepal into Tibet, encompassing parts of Mustang, Manang, Dolpa, and Upper Gorkha. This region is predominantly characterized by marine sedimentary rocks, including limestone, shale, sandstone, and slate, which were deposited in the ancient Tethys Sea prior to the India-Eurasia collision. Despite its significant geographical extent and the growing demand for water to support infrastructure and local livelihoods, systematic groundwater investigation has been historically neglected in this zone within Nepal (Shrestha et al., 2018).

The electrical resistivity method exploits contrasts in the electrical conductivity of subsurface materials to delineate aquifer geometry, depth, and lateral extent, and to trace the boundary between unsaturated and saturated zones. Electrical Resistivity Tomography (ERT), produces a cross-sectional resistivity image from multi-electrode arrays and is now a standard low-cost, non-invasive tool for siting deep tubewells (Loke, 2004).

The study presents the results of an ERT survey at Korala Naka, a Nepal-China border crossing at approximately 4,660 m elevation, undertaken to evaluate the groundwater potential and characterize the subsurface hydrogeological conditions of the Korala Naka area, Upper Mustang, Nepal, using Electrical Resistivity Tomography (ERT).

The application of electrical resistivity methods to groundwater exploration is well established. Early theoretical and practical foundations were laid by Telford et al. (1976, 1990) and Robinson and Coruh (1988), who systematized the relationship between apparent resistivity, electrode geometry, and subsurface lithology, while Reynolds (1997) and Palacky (1987) further catalogued the resistivity signatures of sedimentary, igneous and metamorphic targets under varying saturation conditions. In hard-rock and weathered terrains specifically, Ballukraya et al. (1981) demonstrated that formation resistivity is strongly conditioned by the orientation of the electrode spread and the character of the overlying weathered layer, a finding reflected in the present study's choice of array and profile alignment.

Within Nepal, groundwater geophysics has historically concentrated on the Terai and Siwalik belts, where thick unconsolidated alluvium hosts the country's most productive aquifers. Sharma (1974) produced the first nationwide inventory of groundwater resources, and this was substantially expanded through Terai-focused resistivity and drilling programs reported by Duba (1982) and by the Groundwater Development Consultants (1994) reassessment of irrigation groundwater strategy. At the national scale, Grimmelmann and Upreti (1984) synthesized these and other investigations into a Groundwater Potential Map of Nepal, which classifies the Tethys Himalaya as an area of only local, fracture-controlled groundwater occurrence. The present survey was designed to test directly against site-specific geophysical evidence rather than accept a priori.

The regional geological framework for the Korala area draws on a long history of structural and stratigraphic work in the Thakkhola-Mustang graben. Hagen (1968, 1969) first documented the broad tectonic architecture of the Nepal Himalaya, including the bounding Dangarjong fault system later refined by subsequent workers. Bassoullet and Colchen (1974) and Colchen et al. (1980) established the Tethyan sedimentary stratigraphy of the upper Kali Gandaki (Thakkhola) valley, while Fort et al. (1982) and Colchen (1999) described the structural and sedimentological evolution of the graben fill, comprising more than 870 m of Miocene-to-Pleistocene fluvial, lacustrine, and palustrine deposits. Hurtado et al. (2001) subsequently linked graben development to neotectonic activity on the South Tibetan Detachment System, and Adhikari (2009) provided the most recent sedimentological and provenance synthesis of the Thakkhola and Tetang formations, both drawn upon here for lithological interpretation of the ERT sections.

Dhital (2015) and, more recently, Yoshida et al. (2023) integrated these local studies into the broader regional geology and natural-hazard context of the Kali Gandaki corridor used to frame Section 4 of this article.

Despite considerable geological research in the region, no previous study (geophysical or otherwise) has particularly explored groundwater occurrence in the Nepalese Tethys Himalaya. Furthermore, no exploration or production boreholes have been sunk in this area, therefore there is no direct lithological data to calibrate resistivity estimates. To the authors' knowledge, this is the first site-specific Electrical Resistivity Tomography (ERT) examination focused on groundwater exploration in Nepal's Geological Province. By incorporating Loke's (2000) resistivity-based technique into the existing regional stratigraphic framework, the study presents the first geophysical assessment of groundwater potential in a high-altitude, low-recharge environment that has largely gone overlooked.

High-altitude Trans-Himalayan basins such as Upper Mustang lie in the rain shadow of the Annapurna-Dhaulagiri massif and receive a fraction of the precipitation recorded in the Middle Hills or Terai, leaving communities disproportionately dependent on cryospheric sources. Immerzeel et al. (2010) identified the greater Himalaya as one of the world's principal 'water towers', where downstream water security is tied to glacier and snowpack dynamics that are themselves highly sensitive to warming; Bolch et al. (2012) subsequently documented widespread, though spatially variable, glacier mass loss across the Himalayan arc, and Xu et al. (2009) warned that such melting, combined with rising demand, is already compounding seasonal water stress for mountain communities. Mukherji et al. (2015) further emphasized that Himalayan water availability is not only a climatic issue but a governance and access challenge, with sparsely populated, high-altitude settlements such as those of Lo-Manthang Rural Municipality often left outside formal water-supply planning despite being among the most exposed to scarcity. In the Korala area specifically, the combination of low annual precipitation (~307 mm), negligible monsoon penetration, and reliance on a handful of springs and seasonal meltwater streams, this vulnerability at the local scale and underlines the rationale for identifying an independent, climate-buffered water source.

Groundwater offers a comparatively stable, naturally filtered alternative to surface water in settings where snowmelt and rainfall-fed sources fluctuate seasonally or are absent altogether (Todd & Mays, 2005; Fetter, 2001). Because aquifers buffer short-term climatic variability and typically require far less treatment than surface intakes, systematic exploration to locate and characterize them is a prerequisite for resilient rural and institutional water supply, particularly in remote frontier locations such as Korala where alternative infrastructure is limited. Zohdy et al. (1974) established surface geophysics, and electrical methods in particular, as the standard reconnaissance tool for such exploration because it is non-invasive, rapid to deploy in difficult terrain, and substantially less costly than blind exploratory drilling. In the Nepalese context, groundwater exploration has historically been concentrated in the Terai and Kathmandu Valley, where Shrestha et al. (2016) demonstrated its value not only for locating supply but also for assessing aquifer vulnerability to contamination; by contrast, the Tethys Himalaya has remained essentially unexplored (Grimmelmann & Upreti, 1984), leaving planners without an evidence base for siting decisions. Targeted geophysical exploration, as undertaken in this study, is therefore essential both to reduce the risk of unsuccessful ('dry') drilling in a region where every borehole is costly and logistically difficult to execute, and to generate the first calibration data against which future investigations in this geological province can be compared.

ERT has become one of the most widely applied near-surface geophysical techniques because a single 2-D or 3-D resistivity model can simultaneously resolve stratigraphic boundaries, fracture zones, and moisture content. Griffiths and Barker (1993) demonstrated that multi-electrode 2-D imaging substantially improves resolution of structurally complex ground compared with single-depth vertical soundings, while Dahlin (2001) traced the subsequent evolution of automated, multi-channel DC resistivity instrumentation that made routine 2-D and 3-D surveys practical for engineering and hydrogeological work. Loke et al. (2013) reviewed the maturation of inversion algorithms including the smoothness-constrained least-squares approach used in RES2DINV that now allow rapid, quantitatively robust interpretation of field data of the kind acquired at Korala.

Array-selection studies such as Oyeyemi et al. (2022), who used numerical modeling to evaluate the suitability of different electrode arrays for basement-aquifer characterization, further support the choice of array geometry adopted in the present study. Beyond groundwater exploration, published applications of ERT span saline-intrusion mapping in coastal aquifers, landslide and slope-stability characterization, contaminant plume delineation, archaeological and engineering site investigation, and permafrost/frozen-ground studies in high-altitude and high-latitude terrain the latter being particularly relevant to Trans-Himalayan settings where near-surface freezing can complicate near-surface resistivity response. For deep tubewell siting specifically, ERT's principal value lies in constraining the depth, thickness, and lateral continuity of saturated horizons before committing to drilling, precisely the objective pursued in the present study and consistent with the broader case for electrical methods articulated by Reynolds (1997) and Telford et al. (1990). Similarly, Bienibuor et al. (2025) applied gradient- and Wenner-array ERT to identify sustainable groundwater potential zones in the previously uninvestigated Atebubu municipality of Ghana, underscoring ERT's continued value as a first-pass reconnaissance tool in data-scarce hydrogeological settings.

STUDY AREA

Location and Physiography

The survey site lies at Korala Naka, the fourth Nepal-China border crossing reopened by China (after Rasuwa-Kerung, Tatopani-Khasa, and Yari-Purang), within Ward No. 4 of Lo-Manthang Rural Municipality, Mustang District, Gandaki Province (Fig.1). At 4,660 m, Korala is considered the lowest drivable pass linking the Tibetan Plateau and the Indian subcontinent. Lo-Manthang Rural Municipality covers 727 km² across five wards with a total population of 1,899 (NPHC, 2021), bordered by China on the east, west, and north.

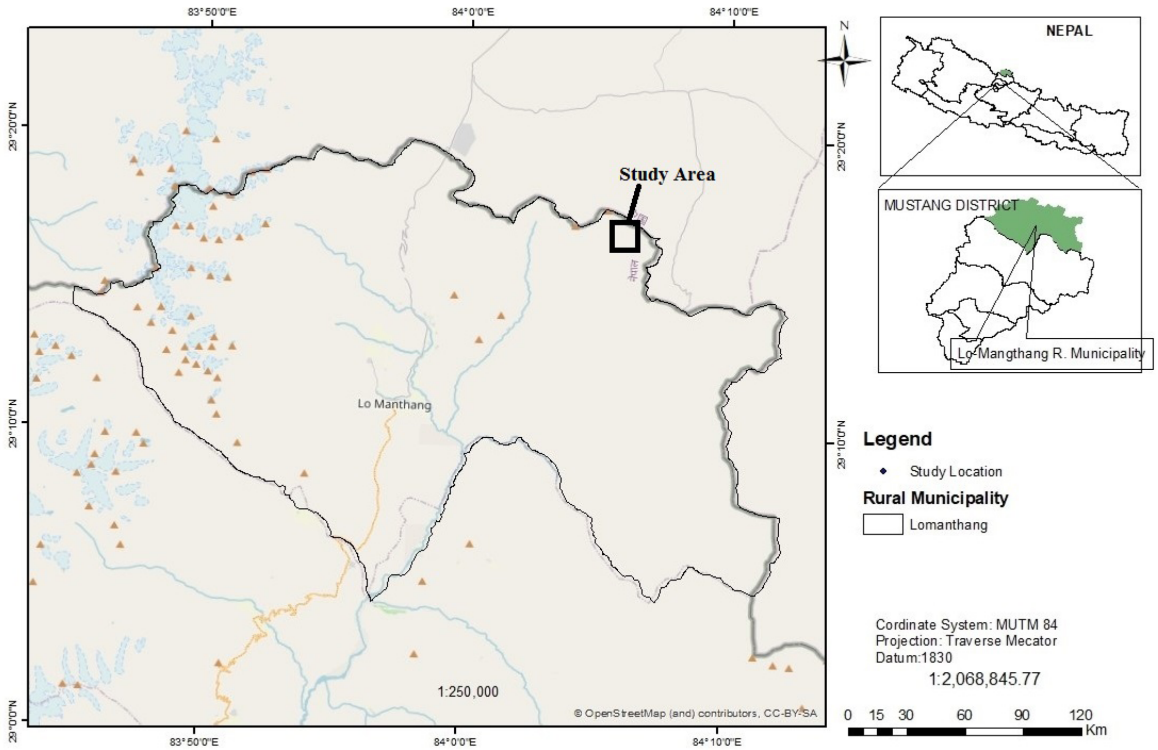

Fig. 1: Location of the study area within Lo-Manthang Rural Municipality, Mustang District, on the Nepal-China border.

Drainage, Climate, and Geomorphology

The Kali Gandaki, the principal river of Mustang, does not pass directly through the Korala area; local drainage is via ephemeral tributary kholas (e.g., Hyujung Khola, Khukyu Khola) fed mainly by seasonal snow and glacial melt, with peak discharge in late spring-early summer. Korala experiences a cold-desert/cold-arid Trans-Himalayan climate with mean annual rainfall of about 307 mm, strong year-round northwesterly winds, winter snowfall, and negligible monsoon influence due to the rain-shadow of the Annapurna-Dhaulagiri range (Table 1). The terrain comprises rugged badlands, wind-eroded ridges, dry valleys, and aeolian sand/silt accumulations shaped by tectonic uplift and fluvio-aeolian erosion of interbedded limestone, sandstone, and shale.

Table 1. Seasonal climatic overview of the Mustang area (source: Department of Hydrology and Meteorology, DHM).

Season	Temperature range	Key features
Winter (Nov–Mar)	–15 to –5 °C (night); below freezing by day	Extremely cold, strong winds, snow-covered
Spring (Apr–May)	–5 to +10 °C	Warming trend, snowmelt begins, cold winds persist
Summer (Jun–Sep)	+5 to +18 °C	Warmer, dry; occasional light monsoon-fringe rain
Autumn (Oct)	0 to +10 °C	Clear skies, cooling, ideal for fieldwork

METHODOLOGY

Principle of Electrical Resistivity

The electrical resistivity method energizes the ground through a pair of current electrodes (C1, C2) and measures the resulting potential difference across a pair of potential electrodes (P1, P2). For a homogeneous half-space, the potential due to a point electrode of resistivity ρ at distance r is $V = \rho I / 2\pi r$ (Fig. 2.), with contributions from multiple electrodes summed algebraically. Apparent resistivity is highly sensitive to lithology, porosity, grain size, water content, salinity, and degree of compaction, and temperature, and differs markedly between dry and saturated formations (Telford et al., 1976; Table 2), which underpins its use for aquifer delineation. Comparable resistivity ranges have been reported in other fractured sedimentary/basement terrains; Bienibuor et al. (2025), for example, observed values of roughly 5-2212 ohm-m across their Ghanaian ERT profiles, with 5-98.6 ohm-m attributed to clay content and 100-506 ohm-m to moderately saturated fractured aquifer zones.

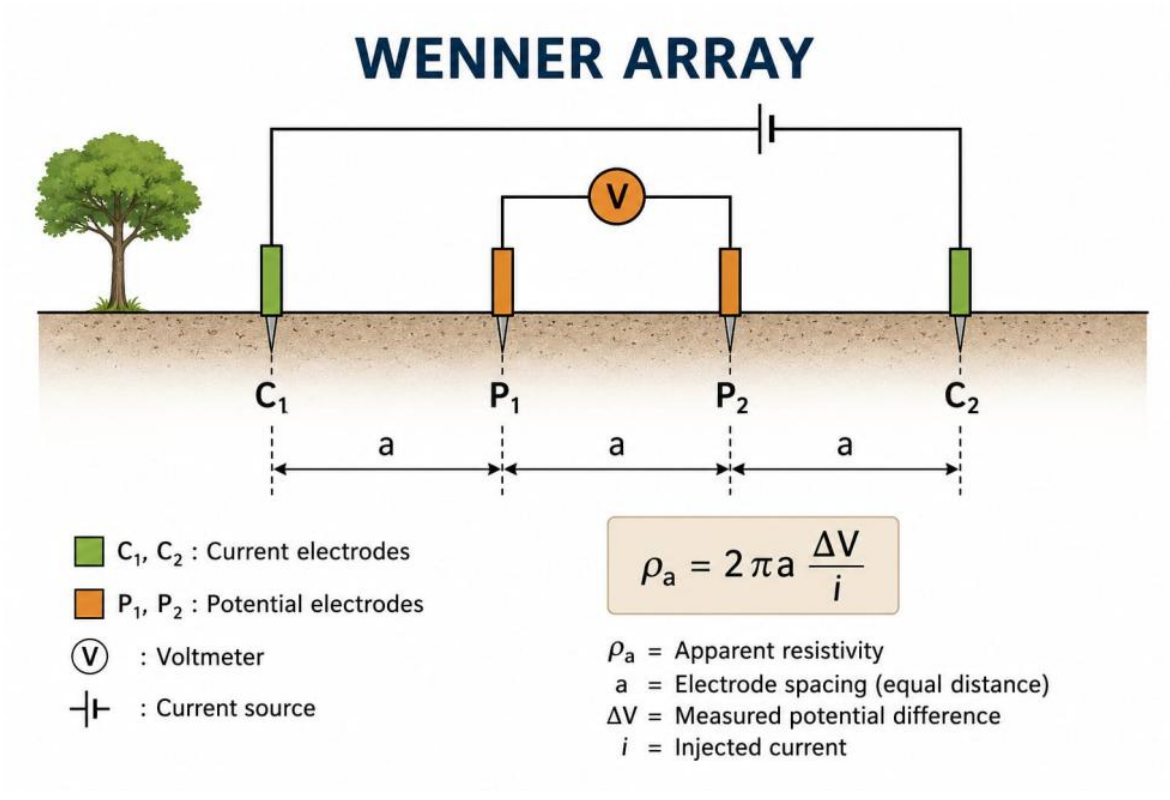

Fig. 2: Wenner array configuration showing electrode arrangement, equal spacing (a), and apparent resistivity calculation.

Table 2. Representative resistivity ranges of common sediments and rock types (after Telford et al., 1976).

Rock type	Resistivity range (ohm-m)
Consolidated shales	$20 – 2 \times 10^3$
Argillites	$10 – 8 \times 10^2$
Conglomerates	$2 \times 10^3 – 10^4$
Sandstones	$1 – 6.4 \times 10^8$
Limestone	$50 – 10^7$
Dolomite	$3.5 \times 10^2 – 5 \times 10^3$
Unconsolidated wet clay	20
Marls	3 – 70
Clays	1 – 100
Alluvium and sands	10 – 800

Field Procedure and Instrumentation

Data were acquired with a GEOMATIVE GD-10 Advanced 2D Plus multi-electrode resistivity/IP imaging system (Geomative Co. Ltd., China), comprising an integrated transmitter, receiver, and microprocessor with automated apparent-resistivity computation and 4-10-fold signal stacking in noisy conditions. Sixty stainless-steel electrodes (30 cm) were deployed along each straight-line profile at 12 m spacing, giving a nominal profile length of 720 m, and were connected via CA30 cables to a central switching mainframe. Measurements were made using all 60 electrodes, four at a time, generating 19 depth levels. The nominal model depth approached approximately 110 m, but this value should not be equated with uniform effective depth of investigation: sensitivity and depth resolution decrease with depth and toward the ends and base of the model. The maximum electrode separation, actual data levels retained after quality control, and the effective depth of investigation should be reported from the acquisition and inversion files. The Wenner configuration was selected for final interpretation because of its strong signal level and stable performance under the field conditions at high altitude. Table 3 lists the coordinates of both profiles, and their spatial alignment relative to the Korala border crossing is shown in Fig. 3.

Depth-of-investigation limitation: With 60 electrodes at 12 m spacing, the nominal maximum spread length is approximately 708–720 m depending on the electrode-count convention used in the acquisition software. The approximately 110 m value is therefore a nominal model extent, not a uniformly resolved depth. The effective DOI should be established from the acquisition geometry and inversion sensitivity/coverage output. In the absence of such a diagnostic, the deepest portion of the model must be treated as less well constrained, and any 150 m drilling target should be considered preliminary and subject to exploratory verification.

Table 3. Selected chainage coordinates for ERT Profile 1 and Profile 2 (full 120 m interval data in the source report); elevations from Google Earth.

Chainage (m)	ERT 1 Lat / Lon/Elevation(m)	ERT 2 Lat / Lon / Elevation(m)
0	29.31769 / 83.98126 / 4608	29.31748 / 83.97959 / 4602
120	29.31828 / 83.98185 / 4603	29.318458 / 83.980059 / 4602
240	29.31898 / 83.98246 / 4604	29.31935 / 83.98074 / 4602
360	29.32035 / 83.98298 / 4602	29.320185 / 83.981498 / 4602
480	29.32125 / 83.98366 / 4600	29.32096 / 83.98244 / 4600
600	29.3222 / 83.98414 / 4601	29.321943 / 83.98298 / 4601
720	29.32268 / 83.98454 / 4601	29.32290 / 83.98328 / 4600

Fig. 3: Alignment of ERT Profile 1 and ERT Profile 2 (100 m apart, north-south orientation) relative to the Korala border crossing, shown on satellite imagery.

Data Processing and Interpretation Framework

Resistivity contours were interpreted in terms of inferred lithology using the regional resistivity–lithology correlation table presented in Table 4, which was developed from previous Groundwater Resources Development Board/Project (GWRDB/GWRDP) groundwater investigations in Nepal. Ideally, these correlations would be checked against borehole logs or exposed geological sections along the ERT profiles. However, no borehole logs, exploratory or production tubewells, or suitable exposed geological sections were available for the investigated profiles. Thus, the resistivity values used for lithological interpretation should be regarded as regional reference values rather than site-specific calibrations. Apparent-resistivity data were screened for outliers using cluster and misfit-histogram analysis, then inverted with RES2DINV (Geotomo Software) to produce topography-corrected 2-D resistivity models after four to five iterations. The RMS misfit provides an indication of how well the calculated model fits the measured data; it does not, by itself, demonstrate geological or hydrogeological reliability because ERT inversion is non-unique. Accordingly, interpretation confidence was assessed qualitatively using the continuity and geometry of anomalies, the regional geological setting, electrode coverage, and the expected decrease in sensitivity at depth. Where available, sensitivity/coverage or DOI information should be shown to identify portions of the sections that are weakly constrained. Because no exploratory or production tubewell exists anywhere in the Nepalese Tethys Himalaya for ground-truthing, the interpretation carries inherent non-uniqueness: overlapping resistivity ranges among dry sand, fractured rock, and clayey silt, generalized (non-site-calibrated) reference values, and multiple resistivity distributions that can fit the same inverted data.

Table 4. Resistivity-lithology correlation used for interpretation (source: GWRDP/GWRDB regional survey experience).

Lithology	Resistivity (ohm-m)
Clay, silt (saturated)	< 50
Silt, fine sand (saturated)	50 – 100
Fine to coarse sand (saturated)	100 – 250
Cobble, pebble, boulder (dry)	> 1000
Cobble, pebble, boulder (saturated)	250 – 1000
Fractured bedrock (saturated)	100 – 1000
Hard/bedrock (saturated)	> 1000

Geological and Hydrogeological Setting

Nepal's Himalaya is divided north to south into the Tethys Himalaya, Higher Himalaya, Lesser Himalaya, Siwalik, and Terai zones, each bounded by major thrust systems (STDS, MCT, MBT, MFT) and each with distinct lithology and deformation history (Upreti, 1999).

The study area lies within the Tibetan Tethys sedimentary series, which occupies the northernmost tectonic zone of the Himalaya as a broad belt of sedimentary rocks (Dhital, 2015). These Tethyan sediments comprise formations ranging in age from Cambrian to Upper Cretaceous (Colchen et al., 1980). In Nepal, the Tibetan Tethys Zone crops out only in limited areas, with the most complete and best-exposed sections occurring in western Nepal along the upper reaches of the Kali Gandaki Valley, commonly known as the Thakkhola Valley (Dhital, 2015).

The Thakkhola Valley is situated north of the main Himalayan Range on its leeward side in central Nepal, and constitutes an Inner Himalayan Basin (Hagen, 1969) located along the upper course of the Kali Gandaki River, locally referred to as the Thakkhola. Sediments within the Thakkhola–Mustang graben accumulated in alluvial fan, braided fluvial, glacio-fluvial, and lacustrine settings (Adhikari, 2009; Adhikari and Wagreich, 2010). Paleocurrent data derived from imbricated pebbles across all basin formations indicate a predominantly southward-directed flow, while microfacies analysis of limestone units points to carbonate deposition in a shallow, flat-bottomed lacustrine environment (Adhikari, 2009).

The Thakkhola–Mustang Graben (Fig. 4.) extends approximately 90 km in length and 20–30 km in width, with a valley floor elevation ranging from 3,000 to 4,000 m, flanked by numerous peaks exceeding 6,000 m (Hagen, 1968). The graben is bounded to the west by the Dangarjong normal fault zone (Hagen, 1968) and to the south by the South Tibetan Detachment System (Hurtado et al., 2001). Its eastern boundary, in contrast, remains poorly defined, while to the north the graben structure diminishes before reaching the Indus–Tsangpo Suture Zone (Dhital, 2015). The graben-fill sequence comprises more than 870 m of Miocene to Pleistocene fluvial, lacustrine, and palustrine sediments, resting unconformably over the underlying Paleozoic and Mesozoic bedrock (Colchen, 1999).

Within this graben-fill, the sediments of the Thakmar Group are subdivided into the Tetang and Thakkhola Formations (Bassoullet and Colchen, 1974). These two formations are, in turn, disconformably overlain by the Sammargaon and Marpha Formations, together with the Lower Terrace deposits of the Kali Gandaki River.

From a hydrogeological perspective, potential aquifers in the Tethys Himalaya are primarily controlled by secondary porosity within fractured/karstified limestone and dolomite, and in fractured sandstone. Shale and slate typically act as aquitards. Recharge is predominantly from snow and glacial meltwater, given the low (~307 mm/yr) and rain-shadow-limited precipitation. This is locally supplemented by percolation from river valleys. To date, no investigation or production tubewell has been drilled on the Nepal side of the Tethys Himalaya. Local reports indicate a single ~100 m tubewell operating on the Chinese side of the border, and a few springs and marshy patches are present within 3 km south of the study site.

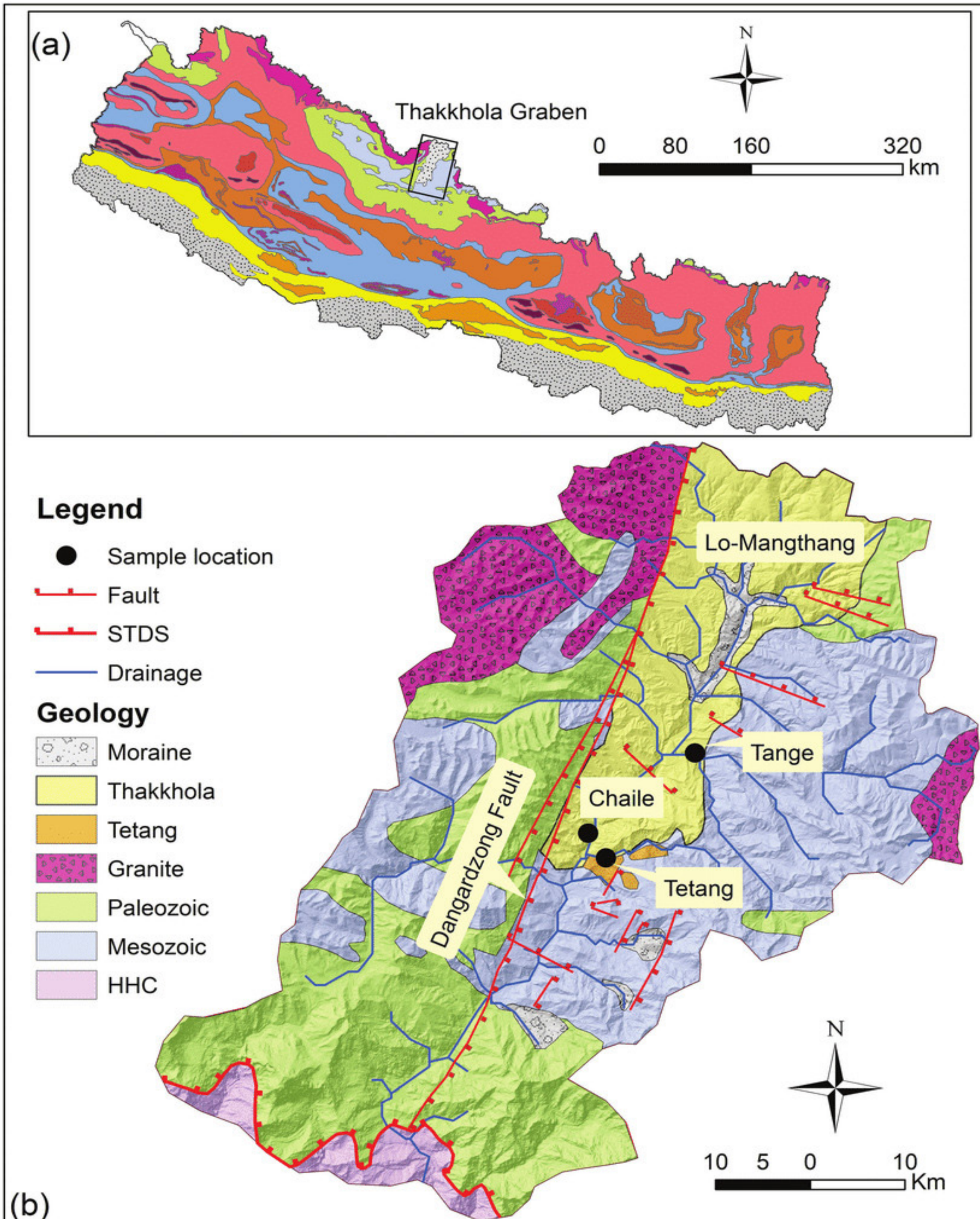

Fig. 4: Schematic geological map of the Thakkhola–Mustang Graben. Source (modified after Adhikari, 2009 and Dhital, 2015).

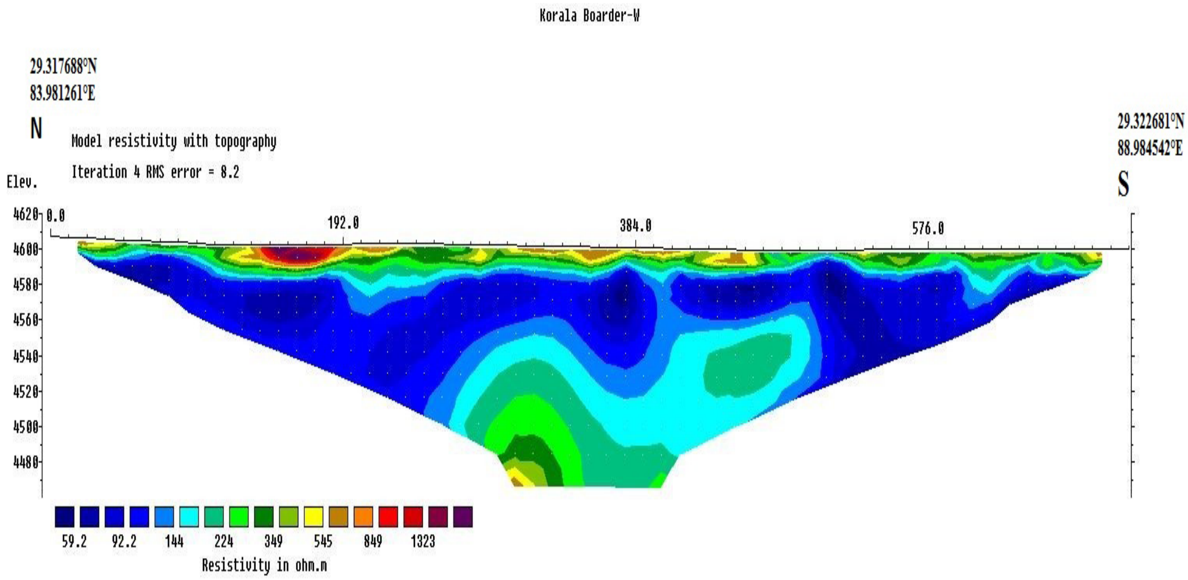

Fig. 5: Topography-corrected inverse resistivity model of ERT Profile 1 (Iteration 4, RMS error = 8.2%).

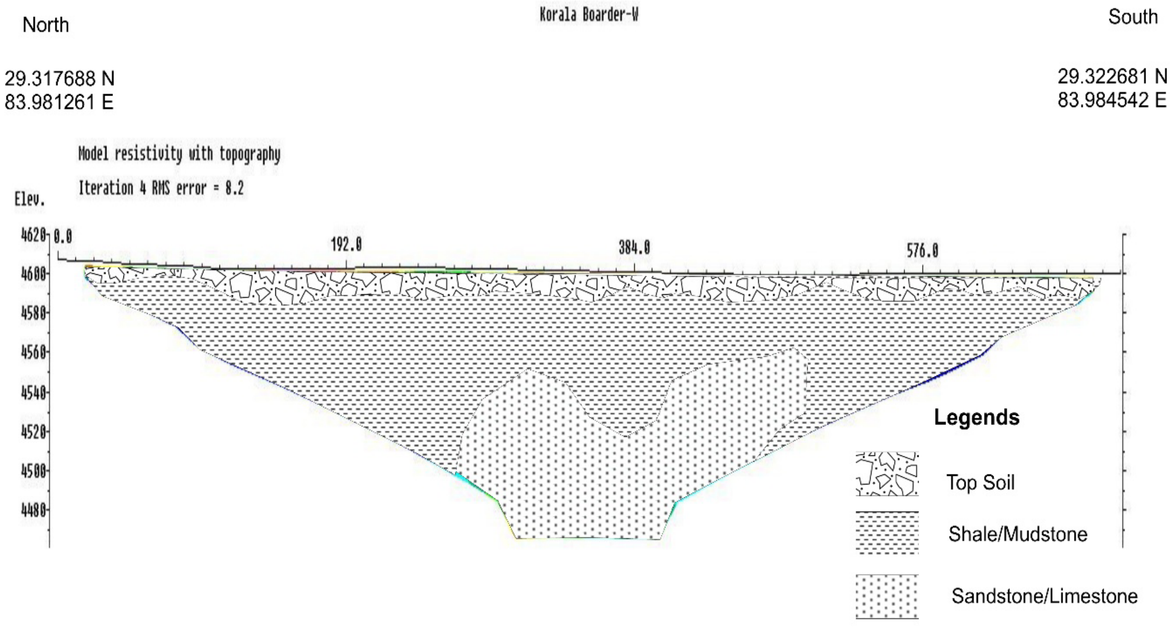

Fig. 6.: Inferred geological section of ERT Profile 1, showing resistivity zones and potential water-bearing formations..

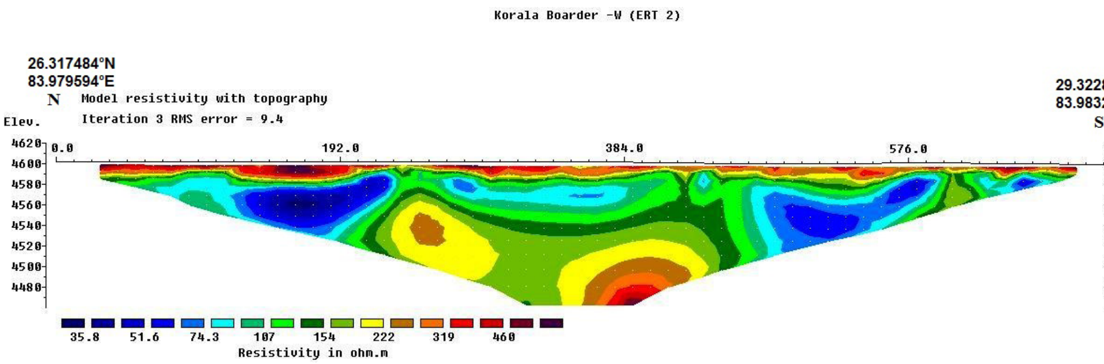

Fig. 7: Topography-corrected inverse resistivity model of ERT Profile 2 (Iteration 3, RMS error 9.4%).

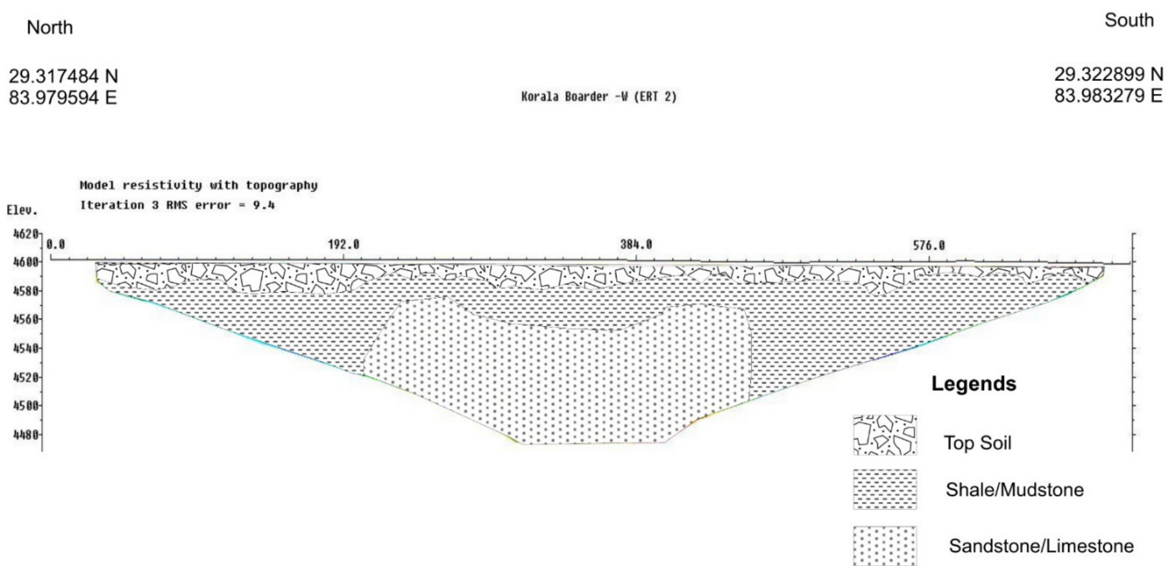

Fig. 8: Inferred geologial section of ERT Profile 2 showing resistivity zones and potential water-bearing formations.

RESULTS AND DISCUSSION

Local Geological Setting of the Korala Border Area

The Korala border area lies within the Tibetan Tethys, also known as the Tethyan Himalaya, the northernmost geological zone of Nepal. The regional geology is dominated by sedimentary rocks and younger deposits associated with the Thakkhola–Mustang graben. Across the wider Mustang region, the graben contains fluvial, alluvial, glacio-fluvial, lacustrine, and palustrine sediments that accumulated during the late Cenozoic. These deposits rest unconformably on older sedimentary bedrock and have been affected by faulting and continued tectonic deformation (Colchen et al., 1980; Colchen, 1999; Adhikari, 2009; Dhital, 2015).

The landscape around Korala consists of dry valleys, eroded slopes, ridges, loose surface material, and locally exposed sedimentary formations. The cold, arid climate and limited rainfall mean that groundwater recharge is likely to depend strongly on seasonal snowmelt and glacier melt. Groundwater may therefore be controlled by fractures, weathered zones, permeable sandstone beds, coarse valley deposits, and contacts between contrasting geological units rather than by one continuous unconsolidated aquifer. Shale and mudstone may restrict groundwater movement where they are intact, but they may store or transmit water where they are fractured, weathered, or interbedded with more permeable layers.

This geological setting provides a reasonable basis for using ERT to identify subsurface electrical contrasts. However, resistivity is not a direct measurement of lithology. Similar values may result from saturated fine-grained sediment, clay-rich material, weathered rock, fractured bedrock, or water with elevated dissolved-ion content. The geological interpretations presented below are therefore plausible models based on the regional setting, not confirmed subsurface observations.

ERT Profile 1

The topography corrected inversion model for Profile 1 extends approximately 720 m along the north south direction (Fig. 5). A thin, relatively resistive zone occurs near the ground surface, with values of approximately 600–1400 Ωm in the most resistive parts. In the dry, high-altitude environment of Korala, this response is consistent with relatively dry surface material, loose debris, weakly weathered sediment, or locally resistive rock fragments. Shallow frozen ground may also contribute to the high resistivity during the survey period.

Below the surface layer, broad low- to moderate-resistivity zones of approximately 50–600 Ωm occur through the central part of the profile. In relation to the local geology, these zones are compatible with moisture-bearing weathered shale or mudstone, fine sandstone, or fractured sedimentary rock. The resistivity data cannot uniquely distinguish these possibilities. In particular, clay-rich material may produce a similarly low response without being a productive aquifer.

A relatively more resistive zone occurs toward the deeper part of the section. This feature may represent less weathered or coarser sediment, sandstone, limestone or relatively competent bedrock. If fractures are present and hydraulically connected, the zone could provide groundwater storage or a pathway for groundwater movement. Because ERT sensitivity decreases with depth, the geometry and significance of this deepest feature are less certain than those of the shallower and central parts of the model (Fig. 6).

ERT Profile 2

Profile 2, located approximately 100 m west of Profile 1, shows a broadly comparable resistivity contrast (Fig. 7). A relatively resistive surface layer overlies low- to moderate-resistivity material in the central and deeper parts of the section. The most conductive zones have resistivities of approximately 30–100 Ωm, while surrounding moderate-resistivity material is approximately 100–200 Ωm or higher, depending on its position within the model.

The similarity between the two profiles suggests that the main electrical contrasts may continue across part of the Korala area. This pattern could reflect laterally persistent sedimentary layers, a weathered zone, or a structurally controlled fractured zone. Local faults, changes in sediment thickness, buried channels, and variations in fracture density may occur between the survey lines.

The deeper low- to moderate-resistivity anomalies in Profile 2 are therefore interpreted as potentially water-bearing geological formations rather than as a confirmed shale–mudstone–sandstone or limestone aquifer sequence. The interpretation is supported by the regional sedimentary geology and the comparable response in Profile 1, but it requires verification through drilling and hydrogeological testing (Fig. 8).

Integrated Geological Interpretation

Together, the two ERT profiles indicate a relatively resistive shallow layer overlying more conductive and electrically variable material. This pattern is compatible with the geological conditions expected at Korala, where dry surface deposits may overlie weathered sediment, fine-grained basin fill, fractured sandstone, shale, mudstone, or older sedimentary bedrock. The results do not support one certain lithological model. Instead, they provide several geological explanations that are consistent with the observed resistivity structure.

Table 5. Geological interpretation of the principal ERT responses at Korala.

ERT response	Possible geological meaning	Hydrogeological implication	Confidence
Relatively high resistivity near surface (600–1400 Ωm)	Dry surface material, loose debris, weakly weathered sediment, or resistive rock/frozen ground	Likely low near-surface water content; may form the unsaturated cover	Moderate
Low resistivity (30–200 Ωm)	Saturated fine sediment, clay-rich material, weathered shale/mudstone, or fractured saturated rock	Potential groundwater occurrence, but productivity is uncertain	Low to moderate
Moderate resistivity (200–600 Ωm)	Fine to coarse sediment, sandstone, weathered bedrock, or partly saturated fractured rock	Possible permeable layer or fracture pathway where connected	Low to moderate
Deeper resistive zones	Less weathered sediment, sandstone, or relatively competent bedrock	May restrict flow, or may transmit water if fractured	Low to moderate

The ERT results are broadly compatible with the geological setting of the Korala border area. The area lies within the Tibetan Tethys, where sedimentary rocks and younger deposits of the Thakkhola–Mustang graben occur together with faults, fractured zones, and variable basin-fill materials. The resistivity sections show a relatively resistive shallow layer overlying low- to moderate-resistivity material. In the local setting, this arrangement may reflect dry surface debris above weathered sediment, fine-grained basin fill, shale or mudstone, fine sandstone, or fractured sedimentary rock.

The lower-resistivity zones are important because groundwater may occur where fine-grained sediment is sufficiently saturated or where fractures provide secondary porosity and pathways for flow. The regional geology supports the possibility of groundwater movement through fractured sandstone, fractured limestone or dolomite, weathered zones, and contacts between contrasting units. Shale and mudstone may act as barriers where they are intact, but they may locally store or transmit water where they are fractured or weathered. For this reason, the anomalies are best described as potentially water-bearing zones rather than as a confirmed aquifer.

Hydrogeological Implications at Korala

The arid, high-altitude climate of Korala limits direct rainfall recharge and increases the importance of seasonal snowmelt and glacier melt. Recharge may occur when meltwater infiltrates through permeable sediment, fractures, valley deposits, or structural discontinuities. The target zones should be tested through exploratory drilling, lithological logging, groundwater-level measurement, water-quality analysis, and pumping or aquifer testing before a production well is designed. A future drilling programme at the Korala would provide the calibration data needed to improve the relationship between resistivity and lithology in the Tethyan Himalaya.

CONCLUSION

Two 720 m Wenner-array ERT profiles at the Korala border area show a broadly similar subsurface electrical structure. A relatively resistive near-surface layer overlies extensive low- to moderate-resistivity zones of approximately 30–350 Ωm. In the context of the local Tethyan Himalayan geology, these zones represent potentially water-bearing fine-grained sediment, weathered material, fractured sandstone, shale, mudstone, or other fractured sedimentary rock.

The results support the use of ERT as a reconnaissance method for identifying and prioritizing groundwater exploration targets. However, the resistivity response is non-unique, and the data do not independently confirm productivity, recharge, hydraulic connectivity, or sustainable yield. The nominal depth approaching 110 m approximately was also interpreted cautiously because the deepest portions of the inversion models are less well constrained.

This study regarded as a preliminary geological and hydro-geophysical assessment rather than a final groundwater-resource evaluation. The identified anomalies may guide exploratory drilling, but lithological logging, groundwater-level monitoring, water-quality testing, and pumping or aquifer testing are required before a deep tubewell is designed or a sustainable water-supply capacity is estimated. These follow-up investigations will determine whether the geological formations at Korala can provide a dependable supply for border infrastructure and nearby communities.

ACKNOWLEDGMENTS

The authors thank the Office Chief and staff of the Water Supply, Water Resources and Irrigation Development Sub-Division Office, Jomsom, Mustang, for commissioning and supporting this study, and the local authorities and residents of Lo-Manthang Rural Municipality for their cooperation and logistical assistance during fieldwork.

AUTHORS' CONTRIBUTIONS

Both authors contributed substantially to the conception and development of this study. The first and corresponding author led the research, including field investigation, data collection, analysis, and preparation of the initial manuscript. The second author contributed to the research design, interpretation of the results, scientific discussion, and critical revision of the manuscript. Both authors jointly contributed to the final development of the manuscript and approved the final version.

CONFLICT OF INTEREST

The authors declare that they have no known financial, personal, or professional conflicts of interest that could have influenced the research or the findings presented in this study.

DATA AVAILABILITY STATEMENT

The data supporting the findings of this study are available from the corresponding author upon reasonable request and can be obtained through direct email communication.

REFERENCES

Adhikari, S. (2009). Sedimentology and provenance of the Thakkhola-Mustang graben, Nepal Himalaya. Unpublished *Ph.D. Thesis*.

Adhikari, B. R., and Wagreich, M. (2010). Provenance evolution of collapse graben fill in the Himalaya—The Miocene to Quaternary Thakkhola-Mustang Graben (Nepal). Sedimentary Geology, 223(1-2), 105-118.

Ballukraya, P.N., Sakthivadivel, R., & Kaliraj, S. (1981). Electrical resistivity investigations for groundwater in hard-rock terrain: a case study. Journal of the Geological Society of India.

Bassoullet, J. P., and Colchen, M. (1974). Stratigraphic succession of the Thakkhola region (Central Nepal).

Bienibuor, A.K., Preko, K., Aning, A.A., Menyeh, A., Wemegah, D.D., Appiah, M.K., & Gyilbag, A. (2025). Application of the electrical resistivity tomography (ERT) method in identifying high groundwater potential sites in the Atebubu municipality of Ghana. Discover Geoscience, 3, 14. https://doi.org/10.1007/s44288-025-00120-x

Bolch, T., Kulkarni, A., Kaab, A., Huggel, C., Paul, F., Cogley, J.G., Frey, H., Kargel, J.S., Fujita, K., Scheel, M., Bajracharya, S., & Stoffel, M. (2012). The state and fate of Himalayan glaciers. Science, 336(6079), 310–314.

Colchen, M., Le Fort, P., & Pecher, A. (1980). Geological map of Annapurna-Manaslu-Ganesh Himal region, Nepal Himalaya.

Colchen, M. (1999). The Thakkhola–Mustang graben in Nepal and the late Cenozoic extension in the Higher Himalayas. *Journal of Asian Earth Sciences*, 17(5-6), 673-689.

Dahlin, T. (2001). The development of DC resistivity imaging techniques. Computers & Geosciences, 27(9), 1019–1029.

Department of Mines and Geology (DMG). (2020, 2023). Geological Map of Nepal / Gandaki Province.

Dhital, M.R. (2015). Geology of the Nepal Himalaya: Regional Perspective of the Classic Collided Orogen. Springer, Heidelberg, 499 p. Springer. https://link.springer.com/book/10.1007/978-3-319-02496-7

Duba, D. (1982). Groundwater resources in the Terai of Nepal. Water and Energy Commission Secretariat Report.

Fetter, C.W. (2001). Applied Hydrogeology (4th ed.). Prentice Hall, 598 p.

Fort, M., Freytet, P., & Colchen, M. (1982). Structural and sedimentological evolution of the Thakkhola-Mustang graben (Nepal Himalayas). Sedimentary Geology.

Griffiths, D.H., & Barker, R.D. (1993). Two-dimensional resistivity imaging and modelling in areas of complex geology. Journal of Applied Geophysics, 29(3–4), 211–226.

Groundwater Development Consultants (GDC). (1994). Reassessment of the Groundwater Development Strategy for Irrigation in the Terai.

Grimmelmann, W.F., & Upreti, S.R. (1984). Groundwater Potential Map of Nepal.

Hagen, T. (1968, 1969). Report on the Geological Survey of Nepal, Vol. 1: Preliminary Reconnaissance. Denkschriften der Schweizerischen Naturforschenden Gesellschaft, Zurich.

Hurtado, J.M., Hodges, K.V., & Whipple, K.X. (2001). Neotectonics of the Thakkhola graben and implications for recent activity on the South Tibetan fault system, central Nepal Himalaya. Geological Society of America Bulletin, 113(2), 222–240.

Loke, M.H. (2000). Electrical Imaging Surveys for Environmental and Engineering Studies: A Practical Guide to 2-D and 3-D Surveys.

Loke, M.H., Chambers, J.E., Rucker, D.F., Kuras, O., & Wilkinson, P.B. (2013). Recent developments in the direct-current geoelectrical imaging method. Journal of Applied Geophysics, 95, 135–156.

Mukherji, A., Molden, D., Nepal, S., Rasul, G., & Wagnon, P. (2015). Himalayan waters at the crossroads: issues and challenges. International Journal of Water Resources Development, 31(2), 151–160.

National Population and Housing Census (NPHC). (2021). Central Bureau of Statistics, Government of Nepal.

Oyeyemi, K.D., Aizebeokhai, A.P., Metwaly, M., Omobulejo, O., Sanuade, O.A., & Okon, E.E. (2022). Assessing the suitable electrical resistivity arrays for characterization of basement aquifers using numerical modeling. Heliyon, 8(5), e09427. https://doi.org/10.1016/j.heliyon.2022.e09427

Palacky, G.J. (1987). Resistivity characteristics of geologic targets. In Nabighian, M.N. (Ed.), Electromagnetic Methods in Applied Geophysics, Vol. 1 (pp. 53–129). Society of Exploration Geophysicists.

Reynolds, J.M. (1997). An Introduction to Applied and Environmental Geophysics. Wiley.

Robinson, E.S., & Coruh, C. (1988). Basic Exploration Geophysics. Wiley, 520 p.

Sharma, C.K. (1974). Groundwater Resources of Nepal. Wonder Printing Press, Kathmandu, 140 p.

Shrestha, A. B., & Aryal, R. (2011). Climate change in the Hindu Kush-Himalayas. Current Opinion in Environmental Sustainability, 3(4), 267-271.

Shrestha, S. R., Tripathi, G. N., & Laudari, D. (2018).Groundwater Resources of Nepal: An Overview. In: Groundwater of South Asia. Springer Hydrogeology.

Shrestha, S., Semkuyu, D.J., & Pandey, V.P. (2016). Assessment of groundwater vulnerability and risk to pollution in Kathmandu Valley, Nepal. Science of the Total Environment, 556, 23–35.

Telford, W.M., Geldart, L.P., & Sheriff, R.E. (1976, 1990). Applied Geophysics (2nd ed.). Cambridge University Press.

Todd, D.K., & Mays, L.W. (2005). Groundwater Hydrology (3rd ed.). Wiley, 636 p.

Upreti, B.N. (1999), "An overview of the stratigraphy and tectonics of the Nepal Himalaya," Journal of Asian Earth Sciences.

Xu, J., Grumbine, R.E., Shrestha, A., Eriksson, M., Yang, X., Wang, Y., & Wilkes, A. (2009). The melting Himalayas: cascading effects of climate change on water, biodiversity, and livelihoods. Conservation Biology, 23(3), 520–530.

Yoshida, M., Ulak, P.D., & Upreti, B.N. (2023). Geology and Natural Hazard along Kaligandaki and Highways Kathmandu-Pokhara-Butwal-Mugling (2nd ed.), 159 p.

Zohdy, A.A.R., Eaton, G.P., & Mabey, D.R. (1974). Application of surface geophysics to ground-water investigations. U.S. Geological Survey Techniques of Water-Resources Investigations, Book 2, Chapter D1.